Design and Experimental Evaluation of a Sensorimotor-Inspired Grasping Strategy for Dexterous Prosthetic Hands

Ting Zhang, *Member, IEEE*, Ning Zhang, Yang Li, Bo Zeng, and Li Jiang

***Abstract*— Stable grasping without slips or crushing is a major challenge for amputees who lose the natural sensorimotor system in dynamically changing daily life environments. Amputees rely largely on visual cues to control the prosthetic hand to complete daily living activities due to a lack of haptic feedback. The human tactile sense can simultaneously feel normal and shear forces. When grasping objects based on the anticipated load conditions, the human hand adjusts the grasping force in real time based on shear force feedback. Here, a sensorimotor-inspired grasping strategy for a dexterous prosthetic hand is proposed to improve grasping performance. The proposed grasping strategy allows the amputee to intuitively control the prosthetic hand. The dexterous prosthetic hand can adaptively adjust the grasp force based on tactile sensory feedback to simultaneously prevent the slipping of objects with unknown shapes, weight, roughness, and softness. Experiments show that the myoelectrical prosthetic hand has grasping force adaptive adjustment and slip prevention ability and provides improved grasping compared to prosthetics with traditional open-loop control.**

***Index Terms*— Dexterous prosthetic hand, grasping, three-axis tactile sensor, slip control.**

I. Introduction

GRASP stability in humans is attributed to the ability to associate tactile (sensory) input with the reflex grasping force (motor). This ability is enabled by the sensorimotor system, which ensures that the human hand has adequate grasp safety margins to prevent objects from slipping or being crushed [1]. Human sensorimotor control includes volitional control and reflexive control [2]. The volitional control process is the high-level cognitive result, while reflexive control is triggered by sensory perception [3]. For example, the process of picking up an egg and relocating it involves both volitional and reflexive controls. The picking up and relocating movements are controlled by the volitional command, while the grasping force adjustment results from the reflexive control, which depends on the sensed properties. For amputees with hand amputation, the sensorimotor system is disturbed, and the bilateral brain-hand loop is disconnected [4].

Electromyography (EMG) pattern recognition-based control [5], [10] allows amputees intuitive control of prosthetic hand motion. Amputees rely largely on visual cues to control the prosthetic hand to complete daily living activities due to a lack of haptic feedback [11]. Prosthetic hand users have heavy visual attention and cognitive burden. In contrast, the human grasp does not need constant visual attention but inherently relies on tactile reflexes to automatically adjust the grasping force [12]. Additional tactile feedback based on electrical stimulation or vibration in the myoelectrical prosthetic hand has been proven to significantly improve grasp performance [6], [13], [16]. However, EMG filters and decoding introduce a time delay to the engineered sensorimotor interface, which connects prosthetic hand movements and muscle contractions. This delay increases the slip frequency when the amputees control the prosthetic hand to grasp objects [17], [18]. Furthermore, the EMG pattern classifier is only able to recognize a few grasp postures and still cannot adjust the grasp based on the object's shape. Effective control methods based solely on EMG are challenging to implement, as the data are insufficient to ensure safe grasping. Amputees control the prosthetic hand to grasp, depending on visual feedback without tactile feedback, and still face instability problems.

Human hand skin includes numerous mechanoreceptors that sense contact information. Picking up an object and putting it back down comprises seven distinct steps: reach, load, lift, hold, replace, unload, and release. Different sets of cutaneous mechanoreceptive afferent types are activated at varying levels (and patterns) with each stage of object handling [17], [19], [20], [21], [22]. During loading and unloading, tactile feedback is needed for the brain to adjust the hand's orientation and grip force to avoid dropping or crushing the held object [22]. If slippage is detected, the hand undergoes a reactive slip prevention

Manuscript received 15 August 2022; revised 24 November 2022 and 14 December 2022; accepted 21 December 2022. Date of publication 23 December 2022; date of current version 2 February 2023. This work was supported in part by the National Key Research and Development Program of China under Grant 2020YFC2007800, in part by the Jiangsu Frontier Leading Technology Fundamental Research Project under Grant BK20192004D, and in part by the Distinguished Professor of Jiangsu Province. *(Corresponding author: Ting Zhang.)*

Ting Zhang and Yang Li are with the Robotics and Microsystems Center, College of Mechanical and Electrical Engineering, Soochow University, Suzhou 215000, China (e-mail: zhangt.hit@gmail.com).

Ning Zhang is with the National Research Center for Rehabilitation Technical Aids, Beijing 100076, China (e-mail: zhangning@nrcrta.cn).

Bo Zeng is with the Laboratory of Aerospace Servo Actuation and Transmission, Beijing Institute of Precision Mechatronics and Controls, Beijing 100076, China (e-mail: zengbo911@163.com).

Li Jiang is with the State Key Laboratory of Robotics and System, Harbin Institute of Technology, Harbin 150001, China.

This article has supplementary downloadable material available at https://doi.org/10.1109/TNSRE.2022.3231972, provided by the authors.

Digital Object Identifier 10.1109/TNSRE.2022.3231972

mechanism to maintain stability. Furthermore, tactile feedback can simultaneously provide the directions and strengths of the applied force [23], [24]. When humans grasp an object, they use anticipated load conditions plus reflexes based on tactile feedback to continuously adjust the applied forces and adjust grip force on objects relative to normal and shear forces at the contact surface [25], [28]. This grasping strategy reduces unnecessary energy consumption and decreases the possibility of damaging the object or causing instabilities as a result of excessive or poorly directed grip forces. However, current myoelectrical prosthetic hands lack this tactile feedback-based reflex grasping to stably grasp soft or fragile objects without dropping or crushing them.

"Incipient slip" and "Gross slip" are two modes of slippage. Only a portion of the contact location lost contact is defined as Incipient slip, while gross motion between the object and the fingers is the Gross slip (or simply "slip") [29]. There have been many studies on the development of tactile sensors for prosthetic hands to detect slips and provide feedback for grasping controllers [30], [35]. Many studies focus on detecting slip by observing the slip displacement using array tactile sensors [34], [36], optical sensors [37], [38], [40], and accelerometers [41] or by observing the time derivative of the pressure sensor [2], [42]. The slip detection and control performance are limited by the resolution of the tactile array. Another popular method to detect slip is based on measuring and analyzing the vibration of the grasping force caused by gross slip [18], [45]. This method cannot detect the slip at the beginning because the vibration must be caused by the slip. However, the initial slip detection is very important for the prosthetic hand to adjust the grasping force in time. If a slip is not detected at the very beginning, the prosthetic hand may not have time to adjust the grasping force to stop it in time. One interesting incipient slip detection method is friction cone-based detection [46], [49]. This method detects incipient slip by observing the measured ratio of the tangential force to the normal force at the contact point by using multiaxial force/tactile sensors. However, there is no dexterous prosthetic hand grasping framework that includes EMG control, incipient slip and gross slip detection, and dynamic adjustment of the grasping force based on three-axis tactile feedback to mimic the human volitional control and reflexive control process of grasping in the activity of daily living (ADL).

Inspired by the fluidity of human grasp control, this paper presents a set of methods that enable hand prostheses to delicately and firmly grasp real-world objects. This study aims to demonstrate the performance of the proposed sensorimotor-inspired grasping strategy of the developed dexterous prosthetic hand, in which the fingertip integrates the developed three-axis tactile sensor [50], [52]. The peculiarities of the proposed approach are its ability to use information extracted from the three-axis tactile sensor array to provide prosthetic hands with real-time stable grasping capabilities depending on tactile feedback rather than relying on constant visual attention.

The main contributions of this paper are summarized as follows.

TABLE I
SPECIFICATIONS OF THE TACTILE SENSOR

Quantity	Value	
	z-axis	x-, y-axis
Force Range	20 N	10 N
Resolution	0.05 N	0.05 N
Sensitivity	0.05N	0.05 N
Average Repeatability	1.5%	1.2%
Average Nonlinearity	3.9%	2.8%
Average Hysteresis	2.4%	2.8%

1) A sensorimotor-inspired grasping framework of a dexterous prosthetic hand is proposed to improve grasping performance. The proposed sensorimotor-inspired grasping strategy can detect both incipient slip and gross slip to adaptively adjust grasp force relative to normal and shear forces to simultaneously prevent slip.

2) To demonstrate the benefits of the proposed sensorimotor-inspired grasping strategy by testing benchtop experiments with different scenes and preliminary human subject validation.

The remainder of this paper is organized as follows. Section II presents the hardware description. Section III presents the framework and details of the proposed sensorimotor-inspired grasping strategy. The benchtop evaluation and preliminary human subject validation of the proposed hardware and grasping strategy are presented in Sections IV and V. Section VI discusses the performance of the proposed prosthetic hand and grasping strategy from the obtained results. Section VII offers conclusions and directions for future work.

II. HARDWARE DESIGN

The prosthetic hand includes five-module fingers, each of which has two links. Both joints of the module finger are driven through one motor with cables, and there is one additional motor to drive thumb abduction/adduction. The maximum fingertip grasping force and joint rotation velocity are 12 N and 80 deg/s, respectively [50]. There is a piezoresistive-principle-based three-axis tactile array with 13 units, in which each tactile unit can measure both the normal force and shear force and covers the five fingertips of the prosthetic hand.

An overview of the proposed prosthetic hand and fingertip three-axis tactile sensor is shown in Fig. 1. There are four fan-shaped top electrodes, as shown in Fig. 1 (b), and one round bottom electrode for each tactile unit. The piezoresistive materials between four fan-shaped top electrodes and one round bottom electrode will work as for resistors to decompose the normal and shear forces from the grasping force on the round mesa, which is mounted on each tactile unit. All 13 tactile arrays are placed to accommodate the shape of the customized fingertip to ensure that there is at least one tactile unit contacting the object for different grasp postures. The diameter of the largest tactile unit, which is fixed on the foremost of the fingertip, is 4 mm, while the other 12 tactile units' diameters are 3 mm [51]. The characteristics of the proposed three-axis tactile sensor are summarized in Table I.

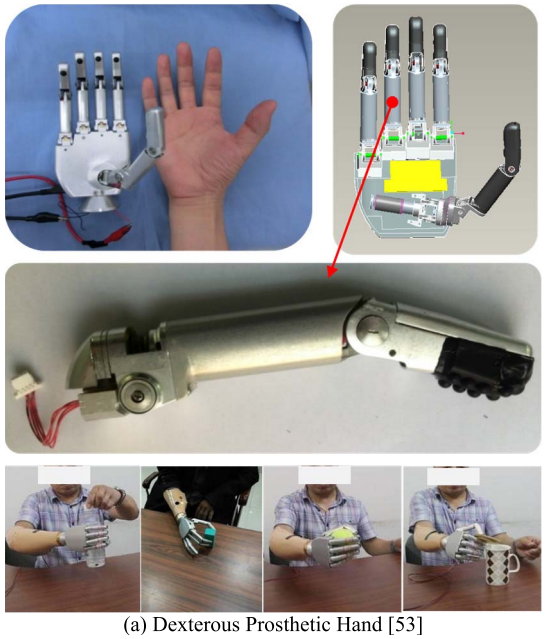

(a) Dexterous Prosthetic Hand [53]

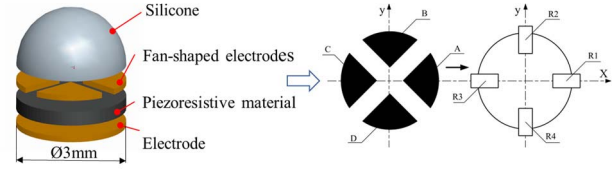

(b) Sensor structure and three-axis forces measure principle [54]

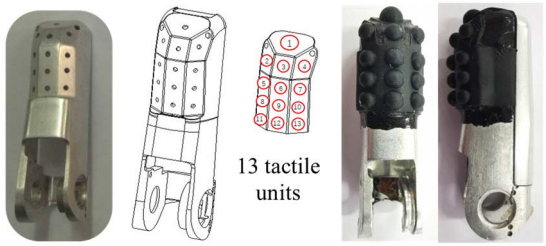

(c) Fingertip structure and tactile sensor placed on the finger [54]

Fig. 1. Experiment platform.

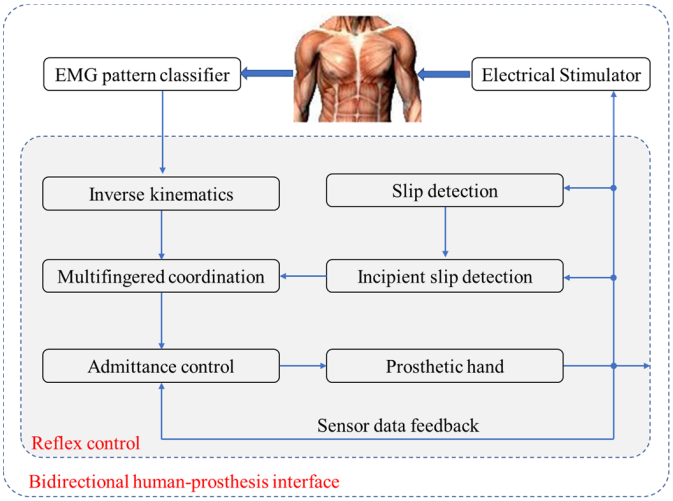

Fig. 2. Framework of the sensorimotor-inspired grasping strategy.

III. Sensorimotor-Inspired Grasping Strategy

A. The Framework of the Sensorimotor-Inspired Grasping Strategy

The goal of the proposed sensorimotor-inspired prosthetic hand's grasping strategy is to rebuild the sensorimotor system to mimic human volitional and reflexive control. The amputee can volitionally control the prosthetic hand based on the EMG signal. And the prosthetic hand also can automatically adjust the applied force based on the three-axis tactile forces feedback.

Fig. 2 shows an overview of the proposed sensorimotor-inspired grasping strategy. It is a hybrid strategy, which includes two loops: bidirectional human-prosthesis interface and reflex control. The bidirectional human-prosthesis interface decodes the grasp intention and grasp posture based on the EMG pattern classifier and feedbacking the grasping force to the user through electrical stimulation. The reflex control is responsible for slip detection and automatically adjusting the grasping force to stabilize grasping.

The pattern classifier decodes the grasping posture from EMG signals and then controls the prosthetic hand based on the intention to grasp. The desired angles of each finger are calculated based on the inverse kinematics and grasping posture. Once contact has been detected through the tactile sensor, the prosthetic hand control is transformed from EMG control to tactile data-driven dynamic grasping control. The prosthetic hand automatically adjusts the grasping force to adapt to the shear force changes (due to the weight change of the object or disturbance) according to the predefined grasping safety margin during the lifting and holding phases. Furthermore, the grasping safety margin is updated in real-time when slippage is detected to prevent further slip. The finger is controlled by the admittance controller to adjust the grasping force in real-time by adjusting the virtual stiffness. The shear-to-normal force ratio was used to adaptively adjust the grasping force based on Coulomb's friction and the grasping safety margin.

B. EMG Pattern Classifier and Electrical Stimulator

The raw EMG signals were collected from six channels of the commercialized dry electrodes integrated with the amplifying circuit (Danyang Prostheses Factory Co., LTD, China) placed on the forearm muscles group, including the extensor pollicis brevis, flexor pollicis longus, extensor indicis proprius, flexor digitorum superficialis (distal), extensor digiti quinti proprius, and flexor digitorum superficialis (proximal). The EMG signals are preprocessed and segmented by overlapping windows. The wavelength (WL) feature that characterizes the signal pattern in each EMG channel is extracted and then fused into one feature vector as the input of the classification algorithm. The pattern classifier categorizes the EMG features into one of the movement classes (i.e., hand open) based on the internal pattern of the EMG data. The classifier can discriminate up to 5 classes: no motion, hand open, power grasp, tip, and tripod. The outputs of the intended movement activate the corresponding prosthetic hand grasp posture for the reflex control.

To detect muscle activation onset quickly and accurately, we applied the Teager-Kaiser Energy Operator (TKEO). TKEO processing was applied to the raw EMG signal as follows:

$$\Psi(n) = x^2(n) - x(n+1)x(n-1) \tag{1}$$

$\Psi(n)$ and $x(n)$ are the TKEO-processed and raw EMG values at the n-th sampling time (n), respectively. The TKEO induces a one-sample time delay in real-time operation. The threshold for the TKEO-processed EMG was obtained as follows:

$$\eta_{tkeo} = \mu + \sigma J \tag{2}$$

μ and σ are the mean and standard deviation of the TKEO-processed EMG during the nonactivated state. J is a multiplier that can be arbitrarily selected. When the rectified TKEO-processed EMG exceeds the threshold (η_{tkeo}), the muscle is considered to be activated.

The support vector machine (SVM) is adopted in this paper as the EMG pattern classifier. The RBF kernel function is used in the classifier. For multimode classification, a one-against-one approach is used. The pattern recognition controller uses an SVM classifier with a segment of 250 ms and a window length of 25 ms, and it runs on the DSP chip (TMS320F2812, Texas Instruments, Texas, USA). The raw analog EMG signals are sampled with a frequency of 200 Hz and 12-bit resolution on the DSP and then filtered with a 20–500 Hz bandpass and 50 Hz notch.

The proposed bidirectional human-prosthesis interface includes the EMG pattern classifier and an electrical stimulator. The one-channel electrical stimulator is designed to achieve a voltage of ±20 V and a sinusoidal waveform output of a maximum of 10 mA. The electrical stimulator can output eight grades of stimulation intensity. The pulse frequency of the electrical stimulator increases from 0 Hz–100 Hz according to the grasping force [53]. The electrode of the electrical stimulator is placed at the upper arm. The voltage electrical stimulus was kept constant, and the current is different depending on the subject's feelings.

C. Reflexive Control

1) Initial Slip Detection and Automatic Grasping Control: The automatic grasping control goal is automatic adjustment of the grasping force to adapt to the shear force changes to prevent slip. On the other hand, to achieve grasp stability, the grasping force must always be situated inside the friction cone at the contact for all fingers, as shown in Fig. 3. And the friction cone will be updated in real-time when a slip occurs. In this method, the stiffness for each finger motion is updated individually so that proper values needed for object motion are synthesized. The prosthetic hand detects the initial slip and automatically adjusts the grasping force through admittance control.

According to Coulomb's law, the normal force f_{normal}, shear force f_{shear} and friction coefficient at the contact point needs to satisfy $|f_{shear}| \big/ |f_{normal}| < \mu_s$ to prevent slipping. The smaller the shear-to-normal force ratio from the friction coefficient, the more stable the grasp is. Soft or delicate

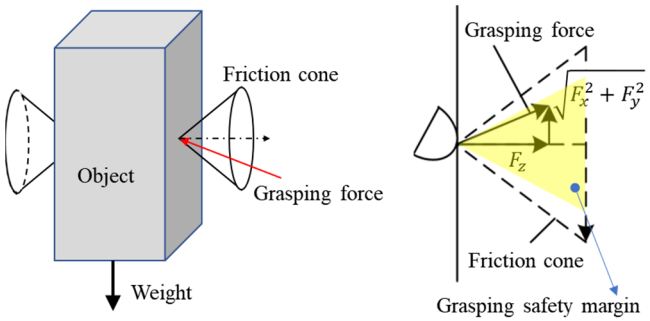

Fig. 3. Schematic of the grasping safety margin. The dome-shaped object represents the sensorized domes on the finger.

objects, which are common in ADLs, may experience large deformations or be crushed when the grasping force increases too aggressively. We chose the tactile unit with the maximum normal force as the effective tactile unit and sent feedback on this tactile unit's three-axis force to the finger controller.

Johansson's work involves analysis of the human grasp resulting in the use of 10% to 40% of the safety threshold based on the material of the object during human grasping of an object [28]. In [47], the ratio of the tangential force to the normal force is calculated in real-time based on the three-axis force collected by the bionic tactile sensor. In addition, the ratio of the tangential force and the normal force is controlled at 0.83 times the maximum static friction coefficient to ensure a stable grasp. We set the friction coefficient μ_s to 0.4, which is suitable for most objects in ADLs. For the initial parameter set, we set the grasping safety margin ξ_p as 0.8 to control each finger's fingertip force to simultaneously prevent slipping and minimize any deformation of the grasped objects. The automatic grasping control goal is real-time adjusting of the grasping force to make the measured ratio of the shear-to-normal forces meet

$$\frac{f_{shear}}{f_{normal}} = \mu_s \cdot \xi_p \tag{3}$$

2) Admittance Control and Stiffness Adjustment: The EMG recognition classifier can only output the grasp patterns. To adapt to different sizes and shapes, the fingers of the prosthetic hand were controlled by admittance control individually. The admittance controller tracking desired joint angles that are calculated through the grasping posture and inverse kinematics of the prosthetic hand. The admittance controller of each finger adjusts the virtual stiffness in real-time to control the grasping force. The admittance controller includes a virtual impedance model working at the outer loop and a trajectory-tracking controller working at the inner loop, in which the stiffness of the prosthetic hand and grasping force can be controlled by adjusting the virtual impedance parameters D and K.

$$\theta_{adj} = \theta_0 - \frac{1}{K + sD} f_{normal} \tag{4}$$

$$K_{T+1} = K_T + \Delta K \tag{5}$$

where θ_0 is the desired finger angle, θ_{adj} is the angle adjustment that is related to the grasping force f_{normal}, s is the Laplace operator, ΔK is the stiffness adjustment, which is

used to determine the stiffness to be applied at the sample time T + 1.

We expect that the reflex grasping force can increase almost instantaneously when a slip is detected to prevent it. However, the object may be crushed or broken if the grasping force increases too aggressively. Furthermore, the grasping force may increase too slowly or not enough to prevent slipping. Therefore, the reflex force amplitude and the time required need to be considered in the design of the stiffness adjustment strategy. The control law for the stiffness adjustment is given by

$$\Delta K = K_P(K_s\mu + K_{sD}\dot{\mu}) \tag{6}$$

$$\mu = \frac{f_{shear}}{f_{normal}} \tag{7}$$

where K_s and K_{sD} are the gains for the ratio of the shear-to-normal force and the ratio of the shear-to-normal force derivation, respectively, K_P is the scale factor.

We use the tactile sensor and angle sensor to estimate the object's stiffness during the contact moment, and then the prosthetic hand grasped the object with a small contact force based on the estimated stiffness:

$$K = \frac{F - F_0}{x - x_0} \tag{8}$$

where F_0, x_0 is the initial grasping force and angle, F is the grasping force mean over n sampling periods, x is the angle mean over n sampling periods.

$$F = \frac{1}{n}\sum_{i}^{i+n} F_i \tag{9}$$

$$x = \frac{1}{n}\sum_{i}^{i+n} x_i \tag{10}$$

The estimated object stiffness to separate object stiffness (<2 N/mm, 2-15N/mm, >15N/mm) and initial grasping force in three levels (0.1-1.5N, 1.5-2.5N, and over 2.5N).

3) Slip Detection and Grasping Safety Margin Update: The initial friction coefficient (μ_s =0.4) and grasping safety margin (ξ_p =0.8) are suitable for most objects, but they are too obtuse and slow for some smooth objects, heavy objects, or when grasping with disturbance. In these cases, the object does slip. Thus, our proposed sensorimotor-inspired grasping controller detects slip based on vibrations and automatically updates the grasping safety margin (from 0.8 to 0.6, adjusted every 0.1) to prevent slip. The slip causes oscillations of both the shear and normal forces. We implemented the Haar wavelet transform analysis of the ratio of the shear-to-normal forces. The slip is distinguished by the threshold. Once the slip is detected, the grasping safety margin ξ_p is updated to increase the sensitivity of the grasping force to the shear force to prevent slip.

The ratio of the shear-to-normal forces of the tactile sensor can be expressed as the linear sum of the scale function and the Haar wavelet function after being decomposed by the Haar wavelet transform.

$$\mu_s(t) = \sum_{n=t_0}^{t_0+N} c_n\varphi\left(2^{j_0}t - n\right) + \sum_{n=t_0}^{t_0+N}\sum_{j=j_0}^{J} d_{j,n}\psi_{j,n}\left(2^{j}t - n\right) \tag{11}$$

where c_n and $d_{j,n}$ are the coefficients, j is the scale coefficient, N is a positive integer number, $\varphi(t)$ is the scaling function, and $\psi(t)$ is the mother wavelet. Define the slip index q as

$$q = \begin{cases} 1 & f_h = d_{j,n}^2 \geq d_s \\ 0 & f_h = d_{j,n}^2 < d_s \end{cases} \tag{12}$$

where d_s is a positive threshold. When high-frequency features of the Haar wavelet $f_h = d_{j,n}^2 \geq d_s$, the $q = 1$, means the slip occurred. We formulate slip detection as a one-class classification problem. The Haar wavelet $DWT = d_{j,n}^2$ is a feature input to the SVM-based one-class classification.

4) Multifingered Coordination: The prosthetic hand is mechanically designed to grasp objects based on the unique configuration of the human hand and the mechanism called "fingers-thumb opposability" [40]. To synchronously adjust all the fingers, all fingers use the same parameter ΔK to adjust their stiffness.

$$\Delta K = \max\left(\Delta K_1\ \Delta K_2\ \ldots\ \Delta K_n\right) \quad i = 1, 2, \ldots, 5 \tag{13}$$

where ΔK_i is the individually updated stiffness of the finger, and i is the finger number.

In this method, the stiffness for each finger motion is updated individually to enable the proper values that are required for the object's motion to be synthesized.

IV. Benchtop Experiments

A. Automatic Grasping Objects

1) Test 1: Grasping Objects With Different Stiffnesses: This experiment demonstrates automatic grasping control of objects with different stiffnesses under a dynamic pushing force. Two objects, hard plastic cups and paper cups, were tested with different stiffness properties. The prosthetic hand was fixed to a frame, and the object was fed to the prosthetic hand to grasp. The manipulandum first grasps and then manually pushes the object in the vertical direction. In this experiment, the grasping safety margin ξ_p was set to 0.8, and then the desired ratio of the shear-to-normal force was 0.32.

As shown in Fig. 4 (a), at the initial stage, the prosthetic hand grasped the object with a small contact force of 0.05 N $\leq f_{normal} \leq$ 0.5 N based on the estimated object stiffness. Once the object is stably grasped, we pushed it downward with a random force. The shear force Fy reflects the pushing force. For the hard plastic cup (Fig. 4 (a)), the prosthetic hand grasped it with an approximately 2 N initial finger force based on the estimated object stiffness is within 2N/mm to 15N/mm. At the interval (0s-t_1), the shear force (Fy) increased due to the weight of the object, and then the grasping force (Fz) increased to keep the ratio of the shear-to-normal force at 0.32. The manual push force was gradually exerted at the interval (t_1-t_2) and interval (t_2-ends), the shear force (Fy) increased with the push force, and then the grasping force increased from 2.8 N to 4.8 N and from 4.8 N to 5.9 N to ensure that the desired ratio of the shear-to-normal force is 0.32 (the grasping safety margin ξ_p is 0.8). Similarly, the prosthetic hand grasped the paper cup with an approximately 1 N initial grasping force based on the estimated object stiffness is small than 2N/mm (Fig. 4 (b)). Then, the grasping

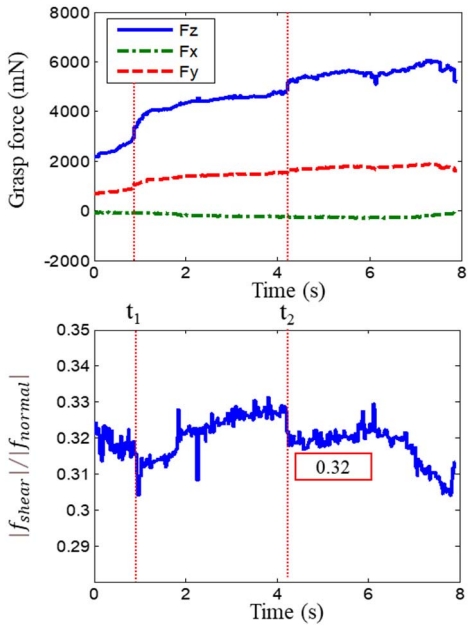

(a) automatic grasping object with high stiffness (hard plastic cup)

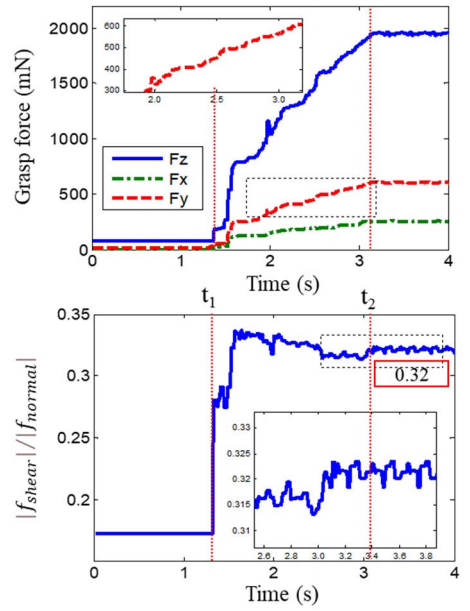

(b) automatic grasping object with low stiffness (paper cup)

Fig. 4. Automatic grasping objects with different stiffness. The manual push force was slowly exerted at the interval (t1-t2) and interval (t3-ends).

force adaptively increases with the push force beginning at t_1 and stopping at t_2. The ratio of the shear-to-normal force is kept at approximately 0.32. In the interval of incipient slip automatic control procedure (t_1-t_2), the prosthetic hand adaptively increases the grasping force (from 0.1 N to 1.9 N).

2) Test 2: Grasping Object With Different Safety Margins: To compare the effectiveness of the grasping safety margin on automatic grasping control, we also conducted a similar experiment with grasping paper cups with different grasping safety margins (Fig. 5 (a)). The incipient slip automatic control experiments are repeated with grasping safety margins ξ_p of 0.7 and 0.6.

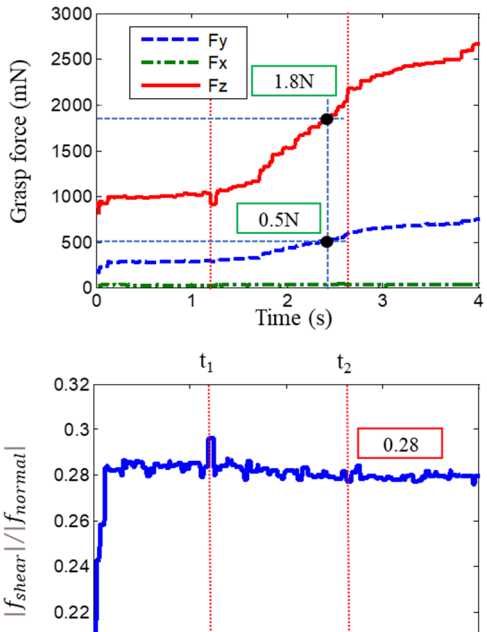

(a) safety margin was set as 0.7

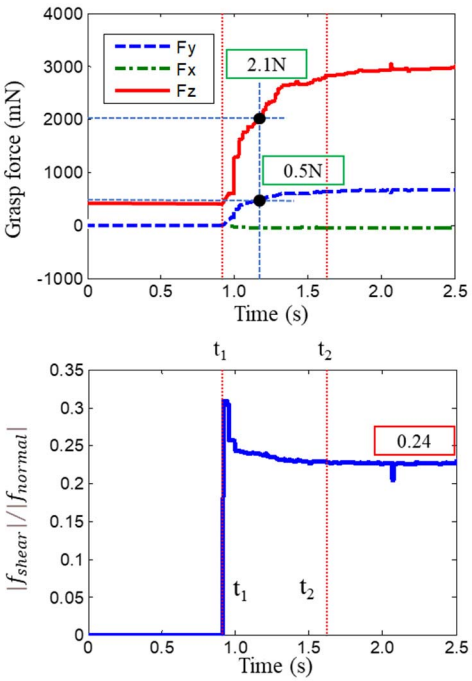

(b) safety margin was set as 0.6

Fig. 5. Automatic grasping object with different safety margins. The manual push force was slowly exerted at the interval (t1-t2) and interval (t3-ends).

As shown in Fig. 5 (a), the grasping force increased at the interval from t_1 to t_2 (from 1 N to 2 N) and the interval from t_2 to 4s (from 2 N to 2.7 N) while the push forces were exerted (the shear force Fy increased from 0.3 N to 0.5 N and from 0.5 N to 0.8 N). The ratio of the shear-to-normal force was approximately 0.28 (the grasping safety margin was set as 0.7) to avoid incipient slip during pushing.

Fig. 5 (b) shows that the grasping force Fz increased from 0.4 N to 3 N when the push force was exerted at the interval from t1 to t2 (Fy increased from 0 N to 0.6 N). The ratio of the shear-to-normal force changed as the push began and was then held at approximately 0.24 (the grasping safety margin was set as 0.6) to avoid incipient slip during pushing. The grasping force is 1.8 N when the shear force is 0.5 N with the grasping safety margin set as 0.7. While the grasping force is up to 2.1 N when the shear force is 0.5 N with the grasping safety margin set as 0.6. The change in grasping force (2.1N) is bigger with the smaller safety margin (0.6).

B. Dynamic Grasping of a Paper Cup

To further demonstrate the grasp and slip prevention ability of the proposed prosthetic hand integrating the three-axis tactile sensor and the proposed sensorimotor-inspired grasping controller, we added rice to the paper cup after the prosthetic hand had stably grasped the paper cup.

As shown in Fig. 6, the shear force increases while adding rice, and the prosthetic hand automatically increases the grasping force to adapt to the shear force changes to prevent incipient slip. As shown in Fig. 6 (b), as the rice was added, the measured shear force increased from 80 mN to 700 mN at the interval from t_1 to t_2, and the grasping force (Fz) correspondingly increased from 100 mN to 2,300 mN. We can see from Fig. 6 (c) that the paper cup slipped from the prosthetic hand at t_2 when the measured shear force (Fy) reached 1.8 N. The cup starts to incipiently slip at the interval from t_1 to t_2 when rice is added. The cup is dropped at t2 due to the weight being too big.

C. Slip Detection and Grasping Safety Margin Update

To evaluate the slip detection and controls, two experiments were conducted at the platform shown in Fig. 1. The first experiment evaluates slip detection by measuring vibrations. In the first experiment, the prosthetic hand stably grasped the paper cup, and then four 50 g weights were dropped into the cup successively. Fig. 7 (a) shows that the ratio of the shear-to-normal force has vibrations, and its high-frequency features of the Haar wavelet were over the threshold (the threshold was set as 0.1) when the object slipped.

The second experiment evaluates the grasping safety margin automatically updated during slip detection. The manipulandum was first grasped, and the weight was added to the plastic cup to make the ratio of the shear force to the normal force rise to 0.32. Then, a 50 g weight was dropped into the cup. Fig. 7 (b) shows that the measured shear force (Fy) increased from 80 mN to 1300 mN (t1), and the grasping force (Fz) correspondingly increased. Slip is detected (t_1 to t_2) by measuring the vibrations of the ratio of the shear-to-normal force, and then the grasping safety margin is updated to 0.7 (the ratio of the shear force to the normal force is updated to 0.28). The grasping force (Fz) increased from 0.8 N to 2.8 N to control the slip and held the ratio of the shear force to the normal force at approximately 0.28.

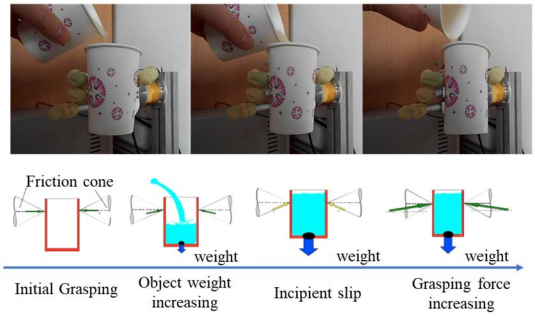

(a)

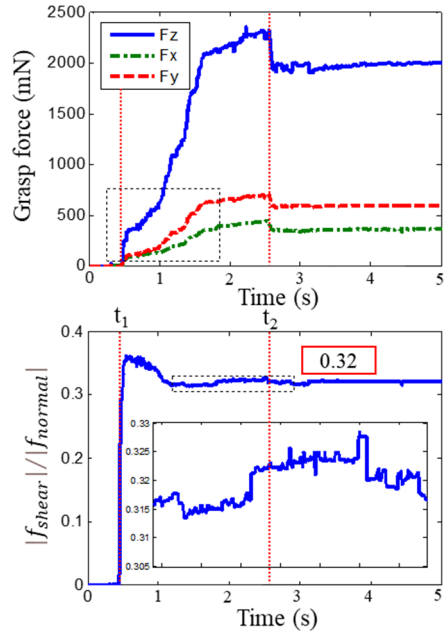

(b) automatic grasping paper cup without slippage

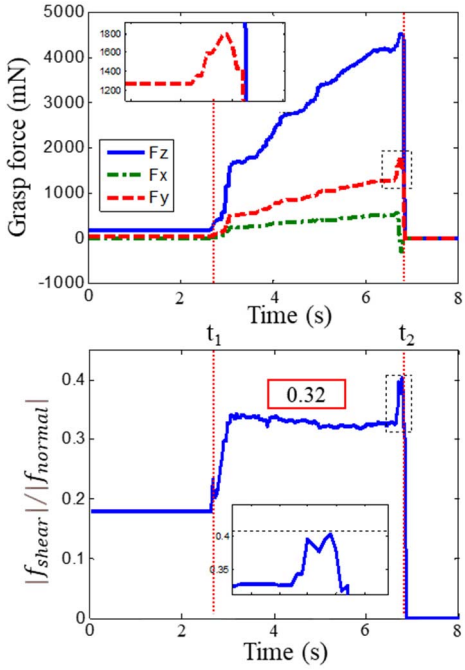

(c) automatic grasping paper cup with the object slipped

Fig. 6. Automatic grasping paper cup with wight increasing. The rice was added into the cup at the interval (t1-t2).

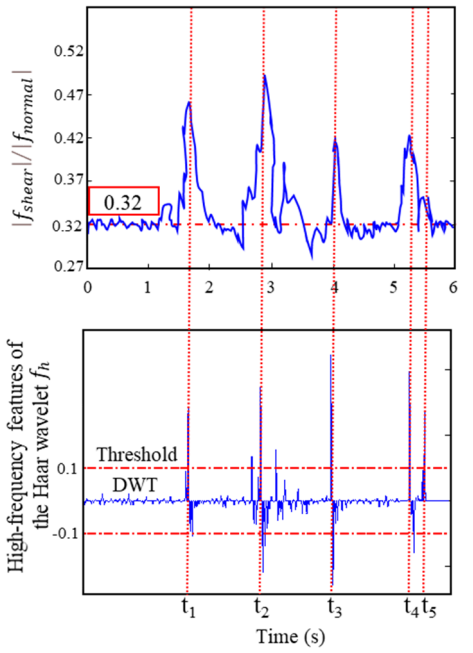

(a) The stacked plot of the slip detection experiment

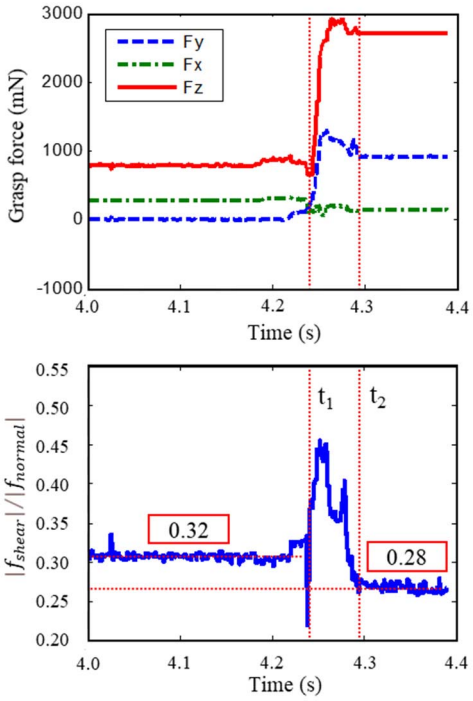

(b) A stacked plot of the slip detection and grasping safety margin update

Fig. 7. Slip detection and control experimental results.

V. Preliminary Human Subject Validation

Five non-disabled subjects (male, age 28.5±6 y.o., weight 78.5±9.9 kg, height 1.76±0.26 m, no prior training with similar devices) were recruited for the experiment to evaluate the performance of the proposed prosthetic hand and the sensorimotor-inspired grasping controller. All subjects signed an informed consent form. The experiments were approved by the Ethical Committee of Soochow University. The six-channel EMG signals, which were measured from six EMG electrodes placed on the forearm, were used to control the prosthetic hand. All five subjects were asked to perform the task in three different control scenarios in two different experiments.

M1: In the first group, we defined modality M1, where the prosthetic hand is controlled by the EMG pattern recognition classifier with position control. The fingers of the prosthetic hand were controlled by position control individually. The position controller tracking desired joint angles that are calculated through the grasping posture and inverse kinematics of the prosthetic hand.

M2: In the second group, we defined modality M2, where the prosthetic hand was controlled the same as in M1, and the grasping force was fed back to the subjects through electrical stimulation [53].

M3: In the third group, we defined modality M3, where the prosthetic hand was controlled by the proposed sensorimotor-inspired grasping controller.

The grasping task is successful when the object is grasped from the table and placed in another location without slipping, breaking, or causing large deformation. The success percentage was defined as the percentage of the number of successful grasping results in the total number of grasping results. The success percentages were statistical analyses by a two-tailed T-test ($P < 0.05$).

Experiment I: A tripod grasp mode was used by the prosthetic hand for all grasping tasks of Experiment I. The EMG electrodes were placed on the subject's left arm, while the prosthetic hand was grasped by the right hand to carry out the pick-lift-replace manipulating tasks during this experiment. Four delicate common objects, paper cups filled with water, strawberries, foam (packing filler), and raw eggs, were chosen for this experiment. For the paper cup filled with water, the subjects were asked to grasp it and then pour the water into another cup. Every subject (total 5 subjects) pick-lift-replace manipulating of each object 5 times (total 100 times, 5 subjects × 4 objects × 5 times).

We can see from Fig. 8 that the success percentage with the proposed control strategies of M3 was higher than those of M2 and M1 for all four objects, especially for the complicated objects. The rate of success for all four objects was greatly increased with M3. The success percentage of the pick-lift-replacement of the paper cup with water increased from 71% to 97%. The success percentage of pick-lift-replacement of the raw egg increased from 50% to 93%. The success percentage of pick lift replacement of the foam increased from 60% to 96%. Strawberry had a high success percentage (from 75% to 91%) for M1, M2, and M3.

Experiment II: Beyond testing the grasping of complicated objects' performance with the tripod grasp mode, we want to evaluate how the proposed system and controller would work on the pick-lift-replace manipulating tasks for real-world soft or delicate objects. In this experiment, three non-disabled subjects and one amputee subject with right transradial amputation (TRA) were asked to pick-lift-replace manipulating 16 different objects with M1, M2, and M3. The object is picked up from a table, and if it is set down at a different location without slippage, crushing, or large deformation, it is considered successful.

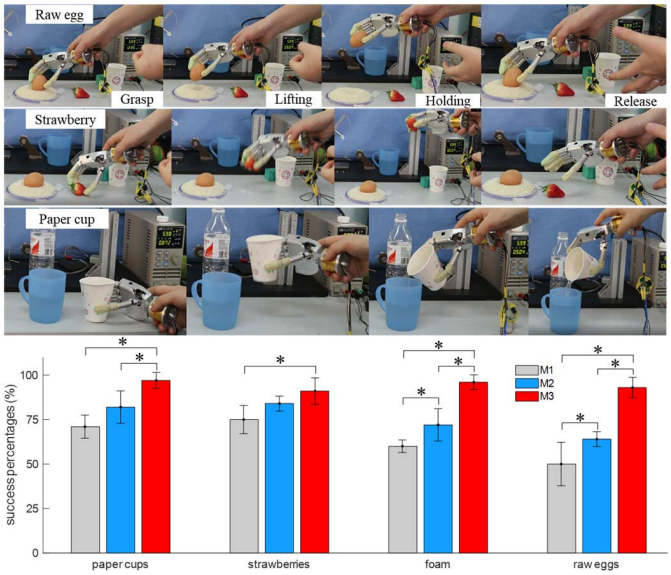

Fig. 8. Experimental results for healthy participants in the experiment. Bars, error bars, and asterisks denoted the means, standard deviations, and statistical significance ($P < 0.05$), respectively.

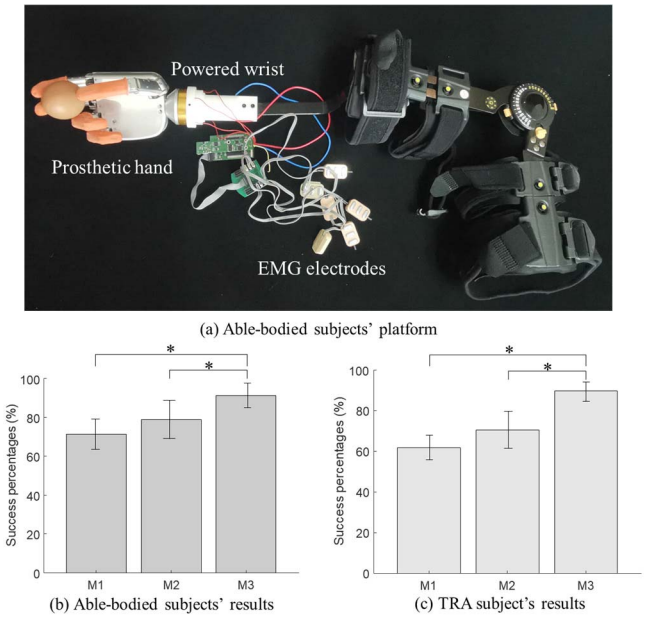

Fig. 9. Experimental results for healthy and TRA participants in experiment II. (a) Prosthetic hand system for non-disabled subjects. (b) Success percentages of the non-disabled subjects. (c) Success percentages of the TRA. Bars, error bars, and asterisks denoted the means, standard deviations, and statistical significance ($P < 0.05$), respectively.

The prosthetic hand was attached to the non-disabled subject's arm through an adapter, and the amputee subject wore the prosthetic hand through a socket, as shown in Fig. 9 (a). The prosthetic hand was controlled by the six EMG electrodes. Common real-world objects with a variety of shapes, weights, roughness, and softness, such as paper cups, plastic cups, raw eggs, strawberries, grapes, sponges, tomatoes, cakes, pies, biscuits, empty juice boxes, mobile phones, light bulbs, hollow paper packaging boxes, small plastic measuring cups, and bananas, were selected for evaluation. Each subject handles 16 objects with 5 repetitions. These objects are grasped with the power, tripod, and tip grasp postures. The success percentage in this experiment is counted based on a total of 240 pick-lift-replace manipulating tasks (3 subjects $\times$ 16 objects $\times$ 5 groups) for the non-disabled subjects and a total of 80 pick-lift-replace manipulating tasks (1 subject $\times$ 16 objects $\times$ 5 groups) for the amputee subject.

The performance of the three control strategies M1-M3 is shown in Fig. 9. The proposed control strategy M3 achieves the highest success percentage across all objects, with a success percentage of 92% for non-disabled subjects and 90% for amputee subjects. The lowest value was in the trial of the experiments with M1 (71% for non-disabled subjects and 62% for amputee subjects). Experiment M2 results (79% for non-disabled subjects and 70% for amputee subjects) in higher percentages than Experiment M1. The success percentages increased from 75% to 96% for the non-disabled subjects and from 64% to 93% for the TRA subject through our proposed method compared with the traditional open-looped EMG controller.

VI. Discussion

As shown in Fig. 4 and Fig.5, all the experiments demonstrated that the proposed sensorimotor-inspired grasping strategy is crucial for grasping force adaptive adjustment for slip prevention and minimizing the deformation of the grasped objects. In the automatic grasping objects with different stiffness experiments (Fig. 4 (a) and (b)), the prosthetic hand automatically increased the grasping force with pushing. Fig.5 validates that the sensitivity of the grasping force to the shear force can be adjusted by changing the grasping safety margin.

In the paper cup dynamic grasping experiment, the grasping force adapted to the weight increased as the rice was filled to prevent slipping. However, the paper cup, as shown in Fig. 6 (c), was dropped with a serious increase in weight. The grasping force is not enough to balance the weight at this moment (at 7 s). Therefore, we increased the sensitivity of the grasping force to the shear force when detecting slip to prevent further slip. As shown in Fig. 7 (a), the high-frequency features of the Haar wavelet for the ratio of the shear-to-normal force are over the threshold when a slip occurs. Furthermore, the grasping safety margin was updated from 0.8 to 0.7 after slippage was detected, as shown in Fig. 7 (b).

In human subject Experiment I, only the tripod grasp mode is used to grasp four delicate objects. At the same time, the prosthetic hand was grasped by the right hand and controlled by the left arm's muscles to carry out the pick-lift-replace tasks during this experiment. This protocol eliminates the need to reduce the loading effects on the EMG pattern classification. As shown in Fig. 8, the proposed sensorimotor-inspired grasping strategy significantly increased the grasp success percentage under similar experimental conditions compared with the traditional open-loop controllers (M1 and M2). Fig. 9 shows that the highest success percentage was obtained in the reach, pick, and lift tasks by the proposed sensorimotor-inspired grasping controller in human subject experiment II.

In summary, this study reports a novel sensorimotor-inspired grasping control framework endowing an engineered sensorimotor system for myoelectrical prosthetic hands. The experiments described above found that the proposed prosthetic hand can automatically adjust the grasping force in real-time to prevent slipping and avoid damaging the objects. Preliminary human subject experiments have shown that our work offers improvements in grasping delicate objects over traditional open-loop control. Furthermore, the proposed controller requires fewer calculations, and all the algorithms, including EMG pattern recognition, run on a DSP chip-based embedded system that is integrated into the prosthetic hand palm. To reduce the size and weight added to the amputee, the prosthetic hand's reliance on external components is minimized.

There have many previous works that tried to rebuild the sensorimotor system for the prosthetic hand, such as human-inspired reflex to autonomously prevent slip of grasped objects rotated with a prosthetic hand [55], sensorimotor-inspired tactile feedback and control of the prosthetic hand [2], neuromimetic event-based detection for closed-loop tactile feedback control of upper limb prostheses [42]. Compared with previous works, the proposed sensorimotor-inspired grasping framework includes EMG control, incipient slip, and gross slip detecting. Furthermore, it allows the prosthetic hand to detect the incipient slip and then dynamically adjust the grasping force to mimic the human reflexive control process of grasping in ADLs. The incipient slip detection will give the prosthetic hand more time to stop the slippage.

However, our work still has limitations. First, the object deformation is judged by the human or drop due to the large deformation during the preliminary human subject validation experiments. This will introduce errors in the statistical results. Second, this study was limited to considering the force/torque equilibrium for stable grasping. Multifingered grasping planning is outside the scope of this study. In addition, this study was limited to adjusting the contact position to achieve new force closure during grasping, which is unstable due to the limits of the prosthetic hand's degrees of freedom. Third, we chose only grasping with the sensor unit with the highest normal force during the experiment. The three-axis tactile sensor array is only integrated at each fingertip, and power grasping without effective tactile unit contacts is not considered in the evaluation. Furthermore, this study was limited to rapid adjustment of the grasping force due to the limits of the finger speeds. To ensure the grasping force and reduce the weight and size, we must compromise between the grasping force and the velocity. The prosthetic hand cannot rapidly increase the grasping force when slippage is detected. Our controller automatically increases the grasping force, adapting to the shear force to prevent slip before it occurs.

VII. Conclusion

In this paper, a sensorimotor-inspired grasping controller is proposed to improve the grasping performance of the prosthetic hand. The advantage of the proposed sensorimotor-inspired grasping control framework is its ability to allow the amputee to intuitively control the prosthetic hand. It also endows the prosthetic hand with the reflex ability to adaptively control the grasping force to simultaneously prevent slipping and minimize the deformation of objects with unknown shapes, weight, roughness, and softness. Experiments found that the myoelectrical prosthetic hand has grasping force adaptive adjustment and slip prevention ability and provides improved grasping compared to prosthetics with traditional open-loop control.

References

[1] R. S. Johansson and K. J. Cole, "Grasp stability during manipulative actions," *Can. J. Physiol. Pharmacol.*, vol. 72, no. 5, pp. 511–524, May 1994.

[2] N. Thomas, F. Fazlollahi, J. D. Brown, and K. J. Kuchenbecker, "Sensorimotor-inspired tactile feedback and control improve consistency of prosthesis manipulation in the absence of direct vision," in *Proc. IEEE/RSJ Int. Conf. Intell. Robots Syst. (IROS)*, Sep. 2021, pp. 6174–6181.

[3] A. B. Schwartz, "Movement: How the brain communicates with the world," *Cell*, vol. 164, no. 6, pp. 1122–1135, Mar. 2016.

[4] A. Ninu, S. Dosen, S. Muceli, F. Rattay, H. Dietl, and D. Farina, "Closed-loop control of grasping with a myoelectric hand prosthesis: Which are the relevant feedback variables for force control?" *IEEE Trans. Neural Syst. Rehabil. Eng.*, vol. 22, no. 5, pp. 1041–1052, Sep. 2014.

[5] A. Furui et al., "A myoelectric prosthetic hand with muscle synergy–based motion determination and impedance model–based biomimetic control," *Sci. Robot.*, vol. 4, no. 31, Jun. 2019, Art. no. eaaw6339.

[6] C. Cipriani, F. Zaccone, S. Micera, and M. C. Carrozza, "On the shared control of an EMG-controlled prosthetic hand: Analysis of user–prosthesis interaction," *IEEE Trans. Robot.*, vol. 24, no. 1, pp. 170–184, Feb. 2008.

[7] D. Farina, "The extraction of neural information from the surface EMG for the control of upper-limb prostheses: Emerging avenues and challenges," *IEEE Trans. Neural Syst. Rehabil. Eng.*, vol. 22, no. 4, pp. 797–809, Feb. 2014.

[8] A. A. Adewuyi, L. J. Hargrove, and T. A. Kuiken, "An analysis of intrinsic and extrinsic hand muscle EMG for improved pattern recognition control," *IEEE Trans. Neural Syst. Rehabil. Eng.*, vol. 24, no. 4, pp. 485–494, Apr. 2015.

[9] N. Jiang, I. Vujaklija, H. Rehbaum, B. Graimann, and D. Farina, "Is accurate mapping of EMG signals on kinematics needed for precise online myoelectric control?" *IEEE Trans. Neural Syst. Rehabil. Eng.*, vol. 22, no. 3, pp. 549–558, May 2014.

[10] A. T. Nguyen et al., "A bioelectric neural interface towards intuitive prosthetic control for amputees," *J. Neural Eng.*, vol. 17, no. 6, Dec. 2020, Art. no. 066001.

[11] D. J. Atkins, D. C. Y. Heard, and W. H. Donovan, "Epidemiologic overview of individuals with upper-limb loss and their reported research priorities," *J. Prosthetics Orthotics*, vol. 8, no. 1, pp. 2–11, 1996.

[12] J. W. Sensinger and S. Dosen, "A review of sensory feedback in upper-limb prostheses from the perspective of human motor control," *Frontiers Neurosci.*, vol. 14, p. 345, Jun. 2020.

[13] S. Raspopovic et al., "Restoring natural sensory feedback in real-time bidirectional hand prostheses," *Sci. Transl. Med.*, vol. 6, no. 222, Feb. 2014, Art. no. 222ra19.

[14] E. D'Anna et al., "A closed-loop hand prosthesis with simultaneous intraneural tactile and position feedback," *Sci. Robot.*, vol. 4, no. 27, Feb. 2019, Art. no. eaau8892.

[15] L. Zollo et al., "Restoring tactile sensations via neural interfaces for real-time force-and-slippage closed-loop control of bionic hands," *Sci. Robot.*, vol. 4, no. 27, Feb. 2019, Art. no. eaau9924.

[16] M. Aboseria, F. Clemente, L. F. Engels, and C. Cipriani, "Discrete vibro-tactile feedback prevents object slippage in hand prostheses more intuitively than other modalities," *IEEE Trans. Neural Syst. Rehabil. Eng.*, vol. 26, no. 8, pp. 1577–1584, Aug. 2018.

[17] R. S. Johansson and G. Westling, "Roles of glabrous skin receptors and sensorimotor memory in automatic control of precision grip when lifting rougher or more slippery objects," *Exp. Brain Res.*, vol. 56, no. 3, pp. 550–564, 1984.

[18] E. D. Engeberg and S. G. Meek, "Adaptive sliding mode control for prosthetic hands to simultaneously prevent slip and minimize deformation of grasped objects," *IEEE/ASME Trans. Mechatronics*, vol. 18, no. 1, pp. 376–385, Feb. 2013.

[19] R. S. Johansson and G. Westling, "Signals in tactile afferents from the fingers eliciting adaptive motor responses during precision grip," *Exp. Brain Res.*, vol. 66, pp. 141–154, Mar. 1987.

[20] R. S. Johansson and G. Westling, "Coordinated isometric muscle commands adequately and erroneously programmed for the weight during lifting task with precision grip," *Exp. Brain Res.*, vol. 71, no. 1, pp. 1–13, Jun. 1988.

[21] R. S. Johansson and G. Westling, "Programmed and triggered actions to rapid load changes during precision grip," *Exp. Brain Res.*, vol. 71, no. 1, pp. 72–86, Jun. 1988.

[22] G. Westling and R. S. Johansson, "Factors influencing the force control during precision grip," *Exp. Brain Res.*, vol. 53, no. 2, pp. 277–284, Jan. 1984.

[23] G. Cadoret and A. M. Smith, "Friction, not texture, dictates grip forces used during object manipulation," *J. Neurophysiol.*, vol. 75, pp. 1963–1969, May 1996.

[24] H. E. Wheat, L. M. Salo, and A. W. Goodwin, "Cutaneous afferents from the monkeys fingers: Responses to tangential and normal forces," *J. Neurophys.*, vol. 103, no. 2, pp. 950–961, Feb. 2010.

[25] J. R. Phillips, R. S. Johansson, and K. O. Johnson, "Representation of Braille characters in human nerve fibres," *Exp. Brain Res.*, vol. 81, pp. 457–472, Aug. 1990.

[26] B. Gesslbauer, L. A. Hruby, A. D. Roche, D. Farina, R. Blumer, and O. C. Aszmann, "Axonal components of nerves innervating the human arm," *Ann. Neurol.*, vol. 82, no. 3, pp. 396–408, Sep. 2017.

[27] J. R. Flanagan, M. K. O. Burstedt, and R. S. Johansson, "Control of fingertip forces in multi-digit manipulation," *J. Neurophys.*, vol. 81, pp. 1706–1717, Apr. 1999.

[28] R. S. Johansson and J. R. Flanagan, "Coding and use of tactile signals from the fingertips in object manipulation tasks," *Nature Rev. Neurosci.*, vol. 10, no. 5, pp. 345–359, 2009.

[29] M. Stachowsky, T. Hummel, M. Moussa, and H. A. Abdullah, "A slip detection and correction strategy for precision robot grasping," *IEEE/ASME Trans. Mechatronics*, vol. 21, no. 5, pp. 2214–2226, Oct. 2016.

[30] M. T. Francomano, D. Accoto, and E. Guglielmelli, "Artificial sense of slip—A review," *IEEE Sensors J.*, vol. 13, no. 7, pp. 2489–2498, Jul. 2013.

[31] Z. Kappassov, J.-A. Corrales, and V. Perdereau, "Tactile sensing in dexterous robot hands—Review," *Robot. Auto. Syst.*, vol. 74, pp. 195–220, Dec. 2015.

[32] A. Saudabayev and H. A. Varol, "Sensors for robotic hands: A survey of state of the art," *IEEE Access*, vol. 3, pp. 1765–1782, 2015.

[33] L. Seminara, P. Gastaldo, S. J. Watt, K. F. Valyear, F. Zuher, and F. Mastrogiovanni, "Active haptic perception in robots: A review," *Frontiers Neurorobotics*, vol. 13, p. 53, Jul. 2019.

[34] J. W. James and N. F. Lepora, "Slip detection for grasp stabilization with a multifingered tactile robot hand," *IEEE Trans. Robot.*, vol. 37, no. 2, pp. 506–519, Apr. 2021.

[35] T. M. Huh, H. Choi, S. Willcox, S. Moon, and M. R. Cutkosky, "Dynamically reconfigurable tactile sensor for robotic manipulation," *IEEE Robot. Autom. Lett.*, vol. 5, no. 2, pp. 2562–2569, Apr. 2020.

[36] J. M. Romano, K. Hsiao, G. Niemeyer, S. Chitta, and K. J. Kuchenbecker, "Human-inspired robotic grasp control with tactile sensing," *IEEE Trans. Robot.*, vol. 27, no. 6, pp. 1067–1079, Dec. 2011.

[37] T. Takahashi et al., "Adaptive grasping by multi fingered hand with tactile sensor based on robust force and position control," in *Proc. IEEE Int. Conf. Robot. Autom.*, Pasadena, CA, USA, May 2008, pp. 264–271.

[38] M. Saen, K. Ito, and K. Osada, "Action-intention-based grasp control with fine finger-force adjustment using combined optical-mechanical tactile sensor," *IEEE Sensors J.*, vol. 14, no. 11, pp. 4026–4033, Nov. 2014.

[39] L. Roberts, G. Singhal, and R. Kaliki, "Slip detection and grip adjustment using optical tracking in prosthetic hands," in *Proc. Annu. Int. Conf. IEEE Eng. Med. Biol. Soc.*, Aug. 2011, pp. 2929–2932.

[40] J. Ueda, A. Ikeda, and T. Ogasawara, "Grip-force control of an elastic object by vision-based slip-margin feedback during the incipient slip," *IEEE Trans. Robot.*, vol. 21, no. 6, pp. 1139–1147, Dec. 2005.

[41] R. J. Lowe, P. H. Chappell, and S. A. Ahmad, "Using accelerometers to analyse slip for prosthetic application," *Meas. Sci. Technol.*, vol. 21, no. 3, pp. 35203–35209, Jan. 2010.

[42] L. Osborn, R. R. Kaliki, A. B. Soares, and N. V. Thakor, "Neuromimetic event-based detection for closed-loop tactile feedback control of upper limb prostheses," *IEEE Trans. Haptics*, vol. 9, no. 2, pp. 196–206, Apr./Jun. 2016.

[43] H. Deng, Y. Zhang, and X.-G. Duan, "Wavelet transformation-based fuzzy reflex control for prosthetic hands to prevent slip," *IEEE Trans. Ind. Electron.*, vol. 64, no. 5, pp. 3718–3726, May 2017.

[44] D. P. J. Cotton, P. H. Chappell, A. Cranny, N. M. White, and S. P. Beeby, "A novel thick-film piezoelectric slip sensor for a prosthetic hand," *IEEE Sensors J.*, vol. 7, no. 5, pp. 752–761, May 2007.

[45] D. Goeger, N. Ecker, and H. Woern, "Tactile sensor and algorithm to detect slip in robot grasping processes," in *Proc. IEEE Int. Conf. Robot. Biomimetics*, Bangkok, Thailand, Feb. 2009, pp. 21–26.

[46] C. Melchiorri, "Slip detection and control using tactile and force sensors," *IEEE/ASME Trans. Mechatronics*, vol. 5, no. 3, pp. 235–243, Sep. 2000.

[47] N. Wettels, A. R. Parnandi, J.-H. Moon, G. E. Loeb, and G. Sukhatme, "Grip control using biomimetic tactile sensing systems," *IEEE/ASME Trans. Mechatronics*, vol. 14, no. 6, pp. 718–723, Dec. 2009.

[48] H. Maekawa, K. Tanie, and K. Komoriya, "Tactile feedback for multifingered dynamic grasping," *IEEE Control Syst. Mag.*, vol. 17, no. 1, pp. 63–71, Feb. 1997.

[49] H. Yussof, M. Ohka, H. Suzuki, and N. Morisawa, "Tactile sensing-based control algorithm for real-time grasp synthesis in object manipulation tasks of humanoid robot fingers," in *Proc. 17th IEEE Int. Symp. Robot Human Interact. Commun.*, Aug. 2008, pp. 377–382.

[50] T. Zhang, L. Jiang, and H. Liu, "Design and functional evaluation of a dexterous myoelectric hand prosthesis with biomimetic tactile sensor," *IEEE Trans. Neural Syst. Rehabil. Eng.*, vol. 26, no. 7, pp. 1391–1399, Jul. 2018.

[51] T. Zhang, L. Jiang, X. Wu, W. Feng, D. Zhou, and H. Liu, "Fingertip three-axis tactile sensor for multifingered grasping," *IEEE/ASME Trans. Mechatronics*, vol. 20, no. 4, pp. 1875–1885, Aug. 2015.

[52] T. Zhang and L. Jiang, "Biomimetic tactile data driven closed-loop control of myoelectric prosthetic hand," in *Proc. IEEE Int. Conf. Robot. Biomimetics (ROBIO)*, Dec. 2018, pp. 1738–1742.

[53] D. Yang, J. Zhao, L. Jiang, and H. Liu, "Dynamic hand motion recognition based on transient and steady-state EMG signals," *Int. J. Humanoid Robot.*, vol. 9, no. 1, Mar. 2012, Art. no. 1250007.

[54] L. Jiang, Q. Huang, D. Yang, S. Fan, and H. Liu, "A novel hybrid closed-loop control approach for dexterous prosthetic hand based on myoelectric control and electrical stimulation," *Ind. Robot, Int. J.*, vol. 45, no. 4, pp. 526–538, 2018.

[55] Z. Ray and E. D. Engeberg, "Human-inspired reflex to autonomously prevent slip of grasped objects rotated with a prosthetic hand," *J. Healthcare Eng.*, vol. 2018, Jun. 2018, Art. no. 2784939.